

"Research Note"

EXPERIMENTAL AND NUMERICAL STUDY OF A TURBULENT AXISYMMETRIC JET IMPINGING ONTO A CIRCULAR CYLINDER IN OFFSET AND NON-OFFSET SITUATIONS*

A. R. TAHAVVOR

Dept. of Mechanical Engineering, Shiraz Branch, Islamic Azad University, Shiraz, I. R. Iran
Email: ath@iaushiraz.net

Abstract– In this study, an experimental and numerical analysis is done to study the flow characteristics of an offset and non-offset axisymmetric jet impingement on a circular cylinder. The purpose of this study is investigation of the behavior of the cutting gas jets and finding the optimum distance between nozzle and cylinder to achieve maximum cutting performance. Finite volume approach is used to solve the governing equations for a turbulent, incompressible jet numerically. According to the literature the suitable turbulence model for this purpose is realizable $k-\epsilon$. Velocity and pressure fields around the cylinder and pressure and shear stress distribution on the cylinder surface are determined for various cases. Also, some experiments are done to validate repeatability of experiments and numerical results. Comparisons between numerical results and experimental measurements validate the accuracy of numerical results. Also, results show that if the horizontal distance between the nozzle outlet and the stagnation point of cylinder is $2.5D$, the shear stress on the cylinder surface has maximum value. Therefore in this situation jet has a maximum performance in cutting procedure.

Keywords– Impinging jet, axisymmetric jet, offset/non-offset impinging, circular cylinder

1. INTRODUCTION

Impinging jets are used in many applications. Low velocity impinging jets are used in paint spraying, heating and cooling applications, etc. High velocity jets are used to cut deposited materials from solid surfaces, for example, cleaning fouled surfaces of cylindrical tubes in heat exchangers.

The heat transfer effect of impinging jets and air flow around bodies has been studied by many researchers such as Refs. [1-9], but from the review of literature it can be observed that the cutting effect of impinging jets has rarely been employed for circular cylinders.

In the present study the flow field of an offset/non-offset turbulent axisymmetric jet which impinges on a circular cylinder is studied and the velocity fields around the cylinder and pressure and shear stress distribution on the cylinder surface for various cases is determined.

2. PROBLEM DEFINITION

The cylinder used in this work is 16 in. long and 1 in. diameter. Also, the diameter of the nozzle outlet is 0.5 in. The air velocity at the nozzle outlet is set to 100m/s. According to environmental conditions, the Mach number is 0.26; therefore the assumption of incompressible fluid flow is acceptable.

Some references state that the critical Reynolds number based on the nozzle diameter and nozzle exit velocity is about 1000 [10], about 3000 [11, 12], or about 14000 [13]. In this study, the Reynolds number is about 64000; therefore the jet used in this study is fully turbulent.

*Received by the editors December 15, 2011; Accepted December 1, 2012.

**Corresponding author

For numerical simulation and experimental measurements two cases are considered:

1- Non-offset situation as shown in Fig. 1a. This case is investigated for $L = 1.5D, 2.0D, 2.5D,$ and $3.0D$ respectively.

2- Offset situation as shown in Fig. 1b. In this case $L = 2.5D$ and offset = $0.2R, 0.4R, 0.6R, 0.8R$ and R . Velocity and pressure fields around the cylinder and pressure and shear stress distribution on the cylinder surface are determined for all cases.

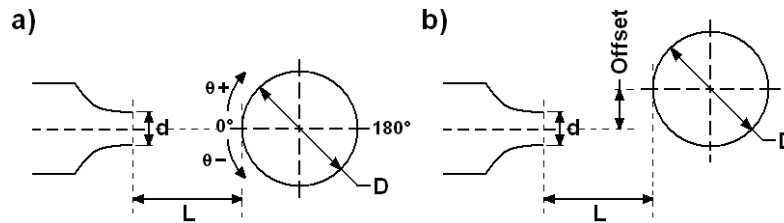


Fig. 1. Orientation of nozzle and cylinder (a) non-offset jet and (b) offset jet

3. GOVERNING EQUATIONS

The time-averaged differential equations governing a steady state and incompressible flow can be written in general form as:

$$U \frac{\partial \Phi}{\partial x} + V \frac{\partial \Phi}{\partial y} + W \frac{\partial \Phi}{\partial z} = \mu \left(\frac{\partial^2 \Phi}{\partial x^2} + \frac{\partial^2 \Phi}{\partial y^2} + \frac{\partial^2 \Phi}{\partial z^2} \right) - \frac{S_{\Phi}}{\rho} \quad (1)$$

Together with the continuity equation

$$\frac{\partial U}{\partial x} + \frac{\partial V}{\partial y} + \frac{\partial W}{\partial z} = 0 \quad (2)$$

Φ may stand for various dependent variables. The particular forms of the individual equations are obtained in Table 1.

Table 1. Summary of equations solved

Equation	Φ	S_{Φ}
x-momentum	U	$-\partial P / \partial x$
y-momentum	V	$-\partial P / \partial y$
z-momentum	W	$-\partial P / \partial z$

The literature such as [14-16] show the inadequacy of standard k- ϵ model in impinging flow situations, but some of them show that realizable k- ϵ model is a suitable model for this purpose [17, 18]. Therefore, in this study realizable k- ϵ model is used as the turbulence model.

It is to be noted that for some simulations standard k- ϵ model is used and results show that this model cannot simulate the flow field accurately, especially in wake region.

4. COMPUTATIONAL PROCEDURE

Equations (1)-(6) are solved numerically, using a code based on a finite volume discretization approach. Several simulations show that the second order upwind is the best momentum discretization scheme for this flow condition. Also, uniform velocity profile is considered for the nozzle outlet velocity as a boundary condition [19]:

$$U = U_{in} \quad (3)$$

As described before, the value of U_{in} is set to 100 m/s.

For determination of kinetic turbulent energy at jet outlet, the following relation is used

$$k = k_{in} = iU_{in}^2 \quad (4)$$

i value is set to 0.04 according to Ref. [19].

According to no-slip condition, the velocity components on cylinder and the supporting walls have been set to zero. A convergence criterion for continuity and momentum equations is set to 10^{-6} and for turbulent equations is set to 10^{-4} . Air is used as a working fluid.

Some grids are tested to obtain grid independent solution. After several tests, it is observed that 12349 grids are sufficiently fine to ensure a grid independent solution.

5. EXPERIMENTAL APPARATUS

The schematic diagram of experimental apparatus is shown in Fig. 2. It consists of:

- Main frame which supports all components of the apparatus.
- Circular cylinder which is made from aluminum with 1 in. diameter and 16 in. length.
- Two Perspex supporting plates which hold the cylinder and allow it to rotate around its axis.
- Nozzle with 0.5 in. outlet diameter.
- Flow measurement devices (which are not shown in the figure) consist of U shaped manometer and air flow meter.
- Air compressor (which is not shown in the figure).

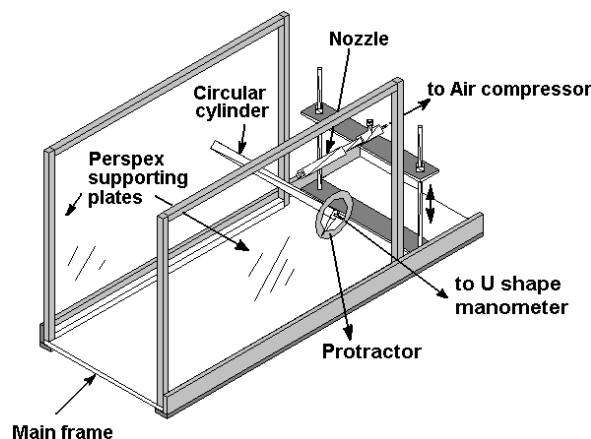


Fig. 2. Experimental apparatus

Air compressor is turned on and tuned until flow meter shows the volume flow rate about 12~13 lit/s. In this case the speed of air at the nozzle outlet is about 100 m/s. Air jet is impinged to the cylinder. Cylinder has a small hole on its surface which is used to determine pressure. This hole is connected to the U shape manometer. For determination of pressure distribution on the cylinder perimeter, the cylinder is rotated around its axis with the increment of 10 degrees and pressure value is recorded for each increment.

6. RESULTS

In this section experimental and numerical results are presented and compared. Pressure distribution is determined numerically and experimentally. Therefore pressure is chosen as a comparison factor between numerical and experimental results. When the validation of the model is confirmed, shear stress distribution is determined numerically.

a) Offset jet, $L=2.5D$

Figure 3 shows the comparison between dimensionless shear stresses on the cylinder for different offsets. The results show that in all cases shear stresses are less than shear stresses in non-offset case except for offset = 0.4R. The reason of this phenomenon is the effect of wake and reversal flow. Applying offset to the jet moves the separation point to the back of the cylinder. Therefore, applying offset to the jet increases the region of the cylinder surface which is affected by the cutting procedure. Only a small region around $\theta = 180^\circ$ is not affected by jet. This region can be cleaned by applying an inclined nozzle. Figures 4, 5 and 6 compare the numerical results with experimental measurements for static pressure on the cylinder perimeter for non-offset jet, offset = 0.4R, and offset = R, respectively. These figures show good agreement between experimental measurements and numerical results and validate the accuracy of numerical results.

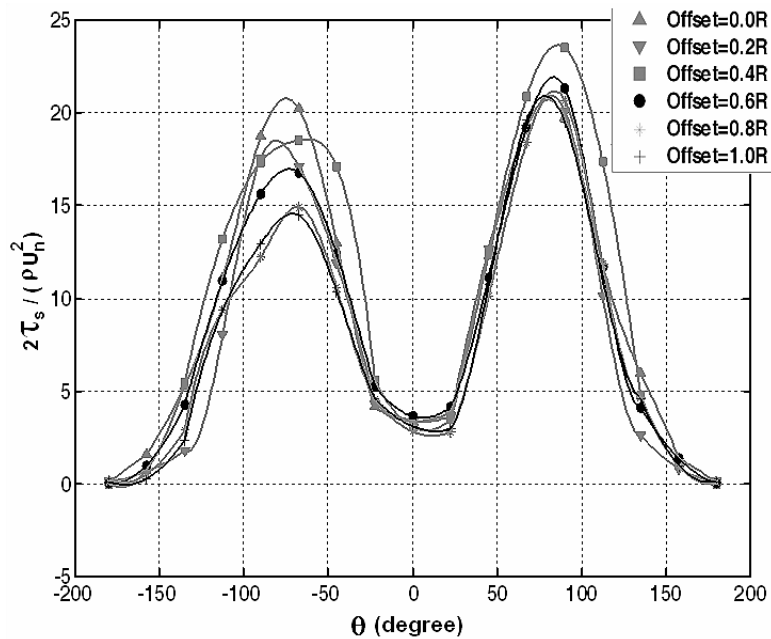


Fig. 3. Shear stress distribution on the cylinder perimeter vis-à-vis the nozzle ($L=2.5D$)

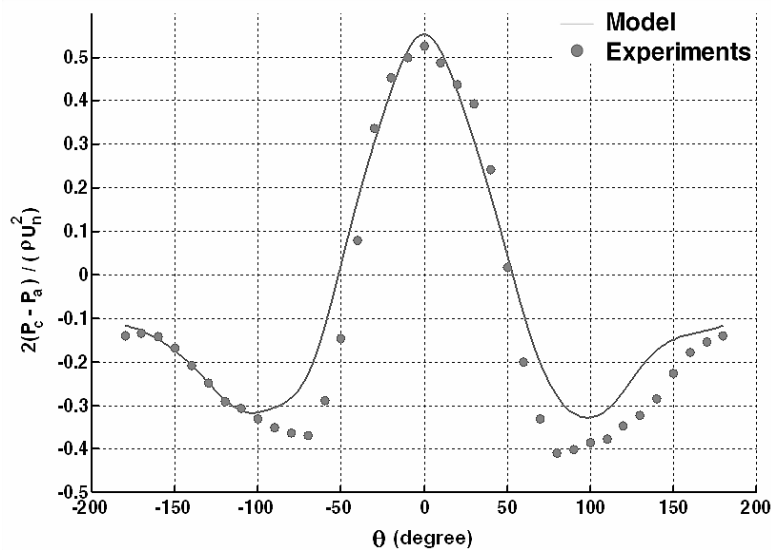


Fig. 4. Static pressure distribution on the cylinder perimeter vis-à-vis the nozzle (non-offset jet, $L=2.5D$)

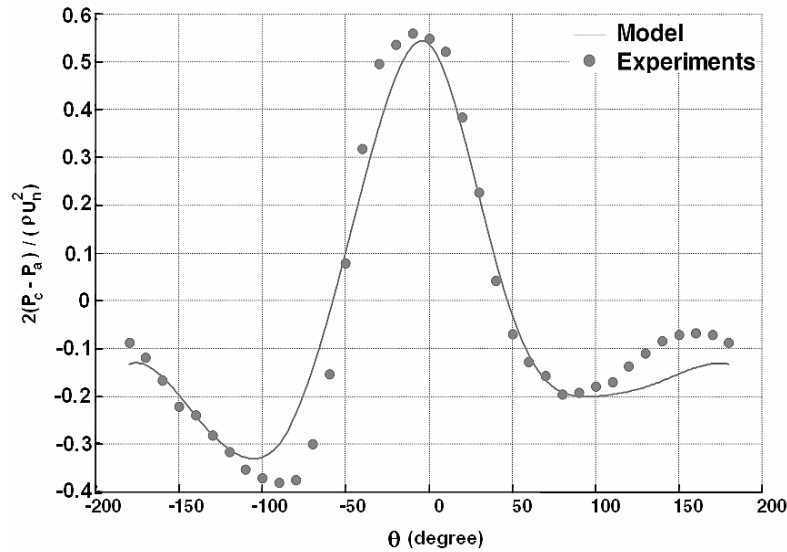


Fig. 5. Static pressure distribution on the cylinder perimeter vis-à-vis the nozzle (offset=0.4R, L=2.5D)

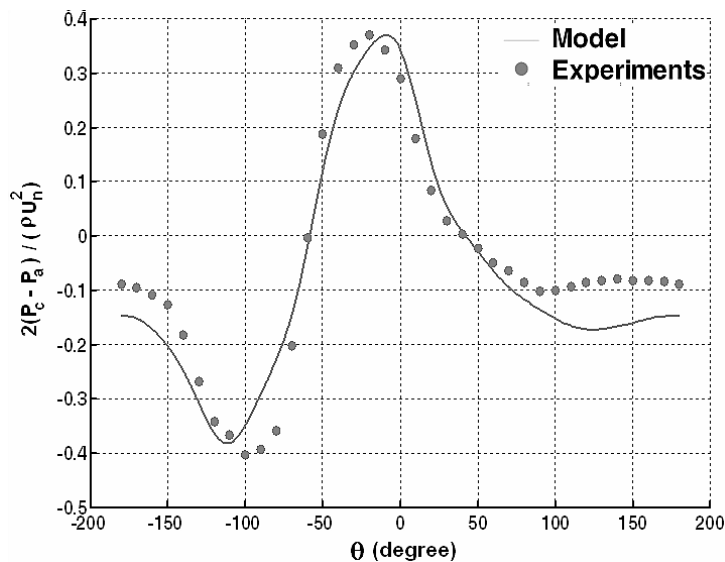


Fig. 6. Static pressure distribution on the cylinder perimeter vis-à-vis the nozzle (offset=R, L=2.5D)

b) Non-offset jet

Figure 7 shows the comparison between shear stresses on the cylinder perimeter at $\theta = 0^\circ$ for $L=2.5D$, $L=1.5D$, $L=2D$ and $L=3D$. This figure shows that maximum shear stresses on the cylinder surface are obtained in the $L=2.5D$ case. Some deviations from symmetry are observed in various curves. These deviations are due to computational errors. It is to be noted that some experiments such as offset = 0, 0.4R and R are repeated twice to validate repeatability of the experiments. Results of these tests are presented in Table 2. According to this table, all the experiments satisfy the repeatability.

Table 2. Value of dimensionless pressure in various tests

	offset = 0	offset = 0.4R	offset = R
1 st experiment	0.533	0.565	0.371
2 nd experiment	0.569	0.593	0.394
3 rd experiment	0.512	0.540	0.357

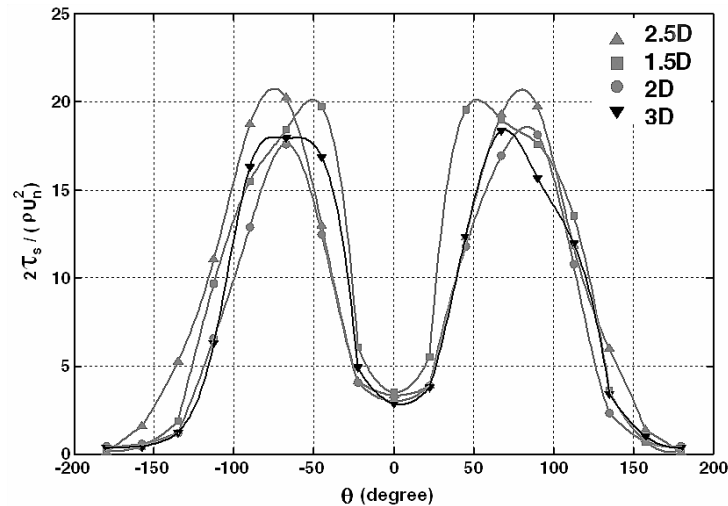


Fig. 7. Shear stress distribution on the cylinder perimeter vis-à-vis the nozzle (non-offset jet)

7. ERRORS AND UNCERTAINTY ANALYSIS

During experiments it was observed that several factors may influence the accuracy of the measurements. Errors may generate from various sources and it is necessary to find the uncertainty of each quantity. These errors and uncertainties are discussed and determined in this section.

Air flow is measured by a flow meter. Specifications of flow meter indicate that the error in measurement is ± 1 lit/sec. Also, pressure is measured by U shaped manometer. The manometer has an error of ± 0.5 cm Hg. Accuracy or discrete uncertainties of these processes are 2% and 8% respectively. The total uncertainty is determined using the Pythagorean summation of discrete uncertainties. Therefore the total uncertainty of pressure measurements is about 6.7%.

8. CONCLUSION

- From the results it can be seen that shear stress in non-offset conditions and for $L=2.5D$ has a maximum value relative to the other cases.
- Applying offset to the jet moves the separation point to the back of the cylinder; therefore, applying offset to the jet increases the region of the cylinder surface which is affected by the cleaning procedure.
- Only a small region around $\theta = 180^\circ$ is not affected by jet.
- For cleaning procedure of heat exchanger's tubes, a high-speed air jet in the cross direction of the cylinder axis which sweeps the cylinder surface can be used.
- As denoted by some researchers, this work also shows that the realizable $k-\epsilon$ model has a good performance in simulation with respect to other turbulence models.

NOMENCLATURE

D	Diameter of cylinder	R	Radius of cylinder
G	Generation rate of k	Re	Reynolds number
L	Distance between nozzle and cylinder	S_ϕ	Source of dependent variable ϕ
P	Pressure	U, V, W	Velocity components
c_1, c_2, c_μ	Constants in turbulence model	u, v, w	Fluctuations of U, V, W
i	Turbulence intensity	x, y, z	Coordinates
k	Kinetic energy of turbulence		

Greek letters

δ_{ij}	Kronecker delta	$\sigma_k, \sigma_\epsilon$	Prandtl numbers for variables k, ϵ
---------------	-----------------	-----------------------------	---

ε	Dissipation rate of k	μ	Viscosity
ν_t	Turbulent viscosity	τ	Shear stress
ρ	Density	Φ, φ	Dependent variable and its fluctuation

Subscript

a	Ambient	s	Cylinder surface
in	Inflow		

REFERENCES

1. Lee, D. H., Chung, Y. S. & Kim, M. G. (1999). Technical note turbulent heat transfer from a convex hemispherical surface to a round impinging jet. *Int. J. Heat Mass Transf.*, Vol. 42, No. 6, pp. 1147-1156.
2. Lee, D. H., Chung, Y. S. & Won, S. Y. (1999). Technical Note The effect of concave surface curvature on heat transfer from a fully developed round impinging jet. *Int. J. Heat Mass Transf.*, Vol. 42, No. 13, pp. 2489-2497.
3. Guerra, D. R. S., Su, J. & Freire, A. P. S. (2005). The near wall behavior of an impinging jet. *Int. J. Heat Mass Transf.*, Vol. 48, pp. 2829-2840.
4. Gradeck, M., Kouachi, A., Dani, A., Arnoult, D. & Boréan, J. L. (2006). Experimental and numerical study of the hydraulic jump of an impinging jet on a moving surface. *Exp. Therm. Fluid Sci.*, Vol. 30, pp. 193-201.
5. Katti, V. & Prabhu, S.V. (2008). Experimental study and theoretical analysis of local heat transfer distribution between smooth flat surface and impinging air jet from a circular straight pipe nozzle. *Int. J. Heat Mass Transf.*, Vol. 51, pp. 4480-4495.
6. Hewakandamby, B. N. (2009). A numerical study of heat transfer performance of oscillatory impinging jets. *Int. J. Heat Mass Transf.*, Vol. 52, pp. 396-406.
7. Koseoglu, M. F. & Baskaya, S. (2008). The effect of flow field and turbulence on heat transfer characteristics of confined circular and elliptic impinging jets. *Int. J. Therm. Sci.*, Vol. 47, pp. 1332-1346.
8. Terekhov, V. I., Kalinina, S. V., Mshvidobadze, Y. M. & Sharov, K. A. (2009). Impingement of an impact jet onto a spherical cavity. Flow structure and heat transfer. *Int. J. Heat Mass Transf.*, Vol. 52, No. 11-12, pp. 2498-2506.
9. Motallebi Hasankola, S. S., Goshtasbi Rad, E. & Abouali, O. (2012). Experimental investigation of the air flow around supported and surface mounted low rise rural buildings. *Iranian Journal of Science and Technology, Transactions of Mechanical Engineering*, Vol. 36, No. M2, pp 143-153.
10. Vickers, J. M. F. (2008). Heat transfer coefficient between fluid jets and normal surfaces. *Industrial Eng. Chemistry*, Vol. 51, pp. 967-972.
11. McNaughton, K. J. & Sinclair, C. G. (1966). Submerged jets in short cylindrical flow vessels. *J. Fluid Mechanics*, Vol. 25, pp. 367-375.
12. Cederwell, K. (1963). The initial mixing on jet disposal into a recipient. Publications Nos. 14 and 15, Division of Hydraulics, Chalmers University of Technology, Goteborg, Sweden.
13. Gordon, R. & Cobonpue, J. (1962). Heat transfer between a flat plate and jets impinging on it. *Int. Developments in Heat Transf, ASME*, Vol. 3, pp. 454-460.
14. Barata, J. M. M., Durão, D. F. G., Heitor, M. V. & McQuirk, J. J. (1992). The turbulence characteristics of a single impinging jet through a crossflow. *Exp. Therm. Fluid Sci.*, Vol. 5, pp. 487-498.
15. Craft, T. J., Graham, L. J. W. & Launder, B. E. (1993). Impinging jet studies for turbulence model assessment - II. An examination of the performance of four turbulence models. *Int. J. Heat Mass Transf.*, Vol. 36, pp. 2685-2697.
16. Nishino, K., Samada, M., Kasuya, K. & Torii, K. (1996). Turbulence statistics in the stagnation region of an axisymmetric impinging jet flow. *Int. J. Heat Fluid Flow*, Vol. 17, pp. 193-201.

17. Fernández, J. A., Elicer-Cortés, J. C., Valencia, A., Pavageau, M. & Gupta, S. (2007). Comparison of low-cost two-equation turbulence models for prediction flow dynamics in twin-jets devices. *Int. Commun. Heat and Mass Transf.*, Vol. 34, pp. 570-578.
18. Balabel, A. & El-Askary, W. A. (2011). On the performance of linear and nonlinear k- ϵ turbulence models in various jet flow applications. *Europ. J. Mech.- B/Fluids*, Vol. 30, pp. 325-340.
19. Kang, S. H. & Greif, R. (1992). Flow and heat transfer to a circular cylinder with a hot impinging air jet. *Int. J. Heat Mass Transf.*, Vol. 35, pp. 2173-2183.